Inorganic Chemistry
Forum Article

Inorg. Chem. **2010**, *49*, 6253–6266 **6253**
DOI: 10.1021/ic902423v

Linkage Isomerization in Heme−NOx Compounds: Understanding NO, Nitrite, and Hyponitrite Interactions with Iron Porphyrins

Nan Xu, Jun Yi, and George B. Richter-Addo*

Department of Chemistry and Biochemistry, University of Oklahoma, 620 Parrington Oval, Norman, Oklahoma 73019

Received December 7, 2009

Nitric oxide (NO) and its derivatives such as nitrite and hyponitrite are biologically important species of relevance to human health. Much of their physiological relevance stems from their interactions with the iron centers in heme proteins. The chemical reactivities displayed by the heme−NOx species (NOx = NO, nitrite, hyponitrite) are a function of the binding modes of the NOx ligands. Hence, an understanding of the types of binding modes extant in heme−NOx compounds is important if we are to unravel the inherent chemical properties of these NOx metabolites. In this Forum Article, the experimentally characterized linkage isomers of heme−NOx models and proteins are presented and reviewed. Nitrosyl linkage isomers of synthetic iron and ruthenium porphyrins have been generated by photolysis at low temperatures and characterized by spectroscopy and density functional theory calculations. Nitrite linkage isomers in synthetic metalloporphyrin derivatives have been generated from photolysis experiments and in low-temperature matrices. In the case of nitrite adducts of heme proteins, both N and O binding have been determined crystallographically, and the role of the distal H-bonding residue in myoglobin in directing the O-binding mode of nitrite has been explored using mutagenesis. To date, only one synthetic metalloporphyrin complex containing a hyponitrite ligand (displaying an O-binding mode) has been characterized by crystallography. This is contrasted with other hyponitrite binding modes experimentally determined for coordination compounds and computationally for NO reductase enzymes. Although linkage isomerism in heme−NOx derivatives is still in its infancy, opportunities now exist for a detailed exploration of the existence and stabilities of the metastable states in both heme models and heme proteins.

Introduction

Nitric oxide (NO) is a well-known biological signaling agent. The well-characterized biological receptor for NO is the heme-containing enzyme-soluble guanylyl cyclase. NO is now known to bind to many heme proteins; some of these interactions are physiologically relevant, and some are not.[1] NO may be oxidized to nitrite under some physiological aerobic conditions, and nitrite can be reduced to NO under some conditions. The hyponitrite dianion is formed during detoxification of NO by some bimetallic metalloenzymes. Indeed, it is becoming more widely accepted that various forms of nitrogen oxides (NOx) may coexist under normal physiological conditions. It is reasonable to assume that the chemical reactions of various heme−NOx species (NOx = NO, nitrite, hyponitrite) are directly related to the NOx binding modes in the reactive species. In this Forum Article, we present and review evidence for the existence of metastable linkage isomers and stable alternate coordination geometries of these heme−NOx species.

Nitrosyl Linkage Isomers

The statistical approach of NO to iron porphyrins could, in principle, involve many forms because NO can rotate as it approaches the metal center. Three limiting forms are sketched in Figure 1. The approach of NO using its N atom at the time of attachment to the metal should, in principle, generate the metal−NO (i.e., "nitrosyl") moiety, and this could either display linear or bent metal−N−O geometries (top of Figure 2). These nitrosyl forms are generally regarded as the ground-state forms of most transition metal−NO compounds.[2] An approach of NO using its O atom at the time of attachment to the metal (middle of Figure 1) should generate the metal−ON (i.e., "isonitrosyl") moiety, as shown at the bottom left of Figure 2. Coppens and co-workers have provided unambiguous crystal structural data for the

*To whom correspondence should be addressed. E-mail: grichteraddo@ou.edu.

(1) Cheng, L.; Richter-Addo, G. B. Binding and Activation of Nitric Oxide by Metalloporphyrins and Heme. In *The Porphyrin Handbook*; Guilard, R., Smith, K., Kadish, K. M., Eds.; Academic Press: New York, 2000; Vol. *4*, pp 219−291.

(2) Richter-Addo, G. B.; Legzdins, P. *Metal Nitrosyls*; Oxford University Press: New York, 1992.

Published on Web 07/12/2010

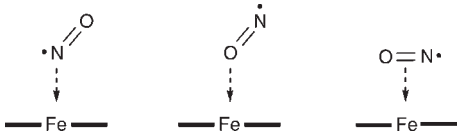

Figure 1. Representative approaches of the NO molecule toward the Fe center in heme proteins.

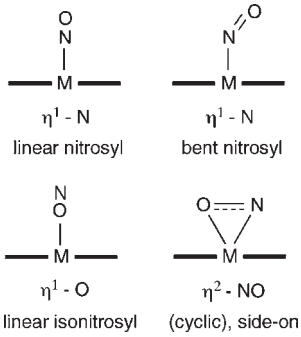

Figure 2. Metal−NO binding modes.

existence of such isonitrosyl species formed during excitation of metal−NO coordination compounds.[3−5] Third, a side-on "belly flop" approach by NO should, in principle, generate the metal−η^2-NO moiety, displaying a side-on attachment of the NO group to the metal center, as shown at the bottom right of Figure 2. Such a binding mode was demonstrated by Coppens for a metastable state of sodium nitroprusside[3] and for a metastable state of CpNi(NO) (Cp = η^5-cyclopentadienyl anion).[6] This side-on NO geometry has also been determined in X-ray crystal structures of the NO adducts of some copper nitrite reductases.[7−9] In this Forum Article, we will use the Enemark−Feltham $\{MNO\}^n$ notation to help describe and classify the metal−NO compounds.[10,11]

Our interest in the linkage isomerization in metal−NO compounds began through a discussion between one of us (G.B.R.-A.) and Philip Coppens at a Poster Session at the 215th National Meeting of the American Chemical Society in Dallas, TX, in April 1998. As a result of this discussion on the possible existence of nitrosyl linkage isomers in nitrosyl metalloporphyrins, we embarked on a three-way collaboration, together with Kimberly Bagley (the team is referred to as the RA−C−B team in this section), to explore the possible generation of such metal−NO linkage isomers in heme models. Our approach was essentially the counterpart to Figure 1, namely, photoexcitation of stable metal−NO (i.e., nitrosyl) porphyrins to generate alternate binding modes of the NO ligand.

Ruthenium Porphyrins. Our team's first attempts to generate nitrosyl linkage isomers in metalloporphyrin derivatives involved the use of ruthenium porphyrins.[12] The reasons for choosing ruthenium were 2-fold. First, we needed to prepare stable and pure (as judged by elemental analysis) six-coordinate mononitrosyl porphyrins. Second, the $\{RuNO\}^6$ class of compounds was a good choice for modeling related group 8 and biologically relevant $\{FeNO\}^6$ congeners. With these in mind, our RA−C−B team examined four $\{RuNO\}^6$ derivatives that differed in trans axial ligation, namely, (OEP)Ru(NO)(O-*i*-C_5H_{11}), (OEP)Ru(NO)(SCH_2CF_3), (OEP)Ru(NO)Cl, and [(OEP)Ru(NO)(py)]$^+$ (OEP = octaethylporphyrinato dianion). Correlated photolysis−IR spectroscopy experiments were then performed.

Irradiation of these compounds ($330 < \lambda < 460$ nm; Xe lamp) as KBr pellets at 20 K for 15 min produced changes in IR absorptions discernible from analysis of the difference IR spectrum. For example, the difference IR spectrum obtained after 15 min of photolysis of (OEP)Ru(NO)(O-*i*-C_5H_{11}) is shown in Figure 3 (bottom trace); the initial ν_{NO} band at 1791 cm^{-1} decreases, and new bands at 1645 and 1497 cm^{-1} become evident.[12] The IR difference spectrum for the ^{15}NO-labeled analogue (OEP)Ru(^{15}NO)(O-*i*-C_5H_{11}) was also obtained (top trace of Figure 3).

The IR data for both the alkoxide (OEP)Ru(NO)(O-*i*-C_5H_{11}) and the thiolate (OEP)Ru(NO)(SCH_2CF_3) compounds are collected in Table 1. Analysis of the IR

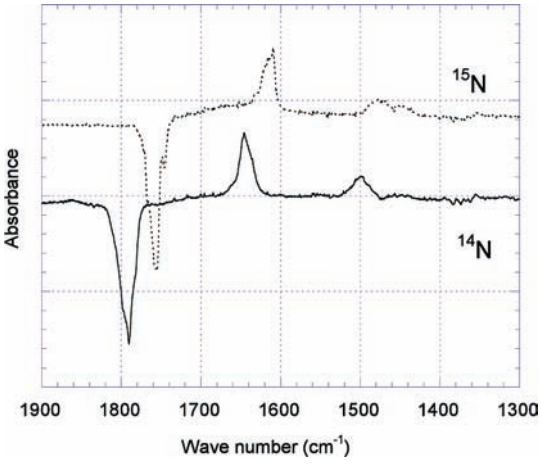

Figure 3. Difference spectra (the spectrum after 15 min of irradiation minus the spectrum prior to irradiation) for the ^{14}NO- (bottom) and ^{15}NO-labeled (top) (OEP)Ru(NO)(O-*i*-C_5H_{11}) compounds.[12]

Table 1. IR Stretching Frequencies (cm^{-1}) and Shifts of N−O Absorption Bands of the Ground State and Metastable States of (OEP)Ru(NO)(O-*i*-C_5H_{11}) and (OEP)Ru(NO)(SCH_2CF_3)[12]

	ν(RuN−O)	ν(RuO−N)	ν(Ru−η^2-N−O)
	(OEP)Ru(NO)(O-*i*-C_5H_{11})		
^{14}N	1791	1645 (−146)	1497 (−294)
^{15}N	1755	1609 (−146)	1480 (−275)
$\Delta[\nu(^{14}N)-\nu(^{15}N)]$	36	36	17
	(OEP)Ru(NO)(SCH_2CF_3)		
^{14}N	1788	1660 (−128)	1546 (−242)
^{15}N	1753	1633 (−120)	1527 (−226)
$\Delta[\nu(^{14}N)-\nu(^{15}N)]$	35	27	19

(3) Carducci, M. D.; Pressprich, M. R.; Coppens, P. *J. Am. Chem. Soc.* **1997**, *119*, 2669–2678.
(4) Fomitchev, D. V.; Coppens, P. *Inorg. Chem.* **1996**, *35*, 7021–7026.
(5) Fomitchev, D. V.; Coppens, P. *Comments Inorg. Chem.* **1999**, *21*, 131–148.
(6) Fomitchev, D. V.; Furlani, T. R.; Coppens, P. *Inorg. Chem.* **1998**, *37*, 1519–1526.
(7) Tocheva, E. I.; Rosell, F. I.; Mauk, A. G.; Murphy, M. E. P. *Science* **2004**, *304*, 867–870.
(8) Antonyuk, S. V.; Strange, R. W.; Sawers, G.; Eady, R. R.; Hasnain, S. S. *Proc. Natl. Acad. Sci. U.S.A.* **2005**, *102*, 12041–12046.
(9) Merkle, A. C.; Lehnert, N. *Inorg. Chem.* **2009**, *48*, 11504–11506.
(10) Feltham, R. D.; Enemark, J. H. *Top. Stereochem.* **1981**, *12*, 155–215.
(11) Enemark, J. H.; Feltham, R. D. *Coord. Chem. Rev.* **1974**, *13*, 339–406.
(12) Fomitchev, D. V.; Coppens, P.; Li, T.; Bagley, K. A.; Chen, L.; Richter-Addo, G. B. *Chem. Commun.* **1999**, 2013–2014.

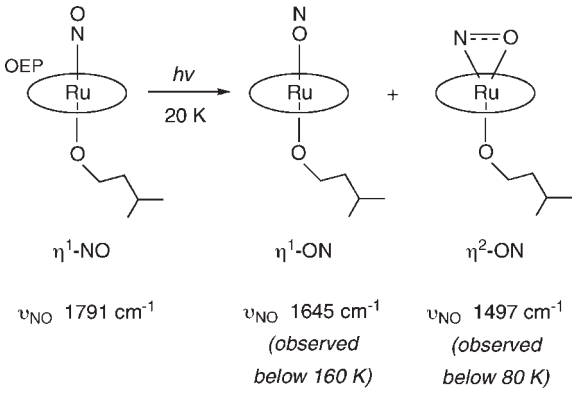

Figure 4. Light-induced generation of metastable nitrosyl linkage isomers during irradiation of (OEP)Ru(NO)(O-*i*-C_5H_{11}) as a KBr pellet.[12]

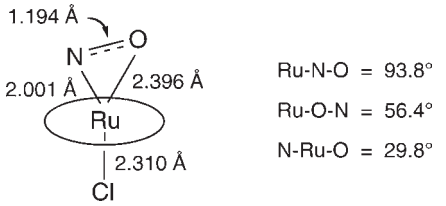

Figure 5. Optimized geometry of the metastable side-on nitrosyl linkage isomer of (OEP)Ru(NO)Cl.[13]

spectral changes suggested that photolysis of these compounds generated metastable η^1-O and η^2-NO linkage isomers, as shown in Figure 4, in low observed yields (1−1.5%).[12] This conclusion of photoinduced isomerization of the RuNO fragment to the linkage isomers was supported by the following: (i) photolysis at 20 K did not produce free NO (ν_{NO} 1880 cm^{-1}); (ii) the photogenerated bands were ^{15}N-shifted in the Ru−^{15}NO derivatives and thus associated with ν_{NO}; (iii) warming the photolyzed samples back to room temperature restored the parent nitrosyl bands, indicating that the photoinduced reaction was thermally reversible and that the photoproducts were indeed metastable species; (iv) the ν_{NO} spectral shifts were similar to those recorded for other metastable nitrosyl linkage isomers in coordination compounds of iron, ruthenium, osmium, and nickel.

Further support for the side-on η^2-NO linkage isomer in the seven-coordinate ruthenium porphyrin was later provided by a density functional theory (DFT) calculation by Ghosh (using the PW91 exchange-correlation functional and triple-ζ plus polarization Slater-type basis sets) on an unsubstituted porphine model for the experimentally observed[12] isomer formed during photolysis of (OEP)Ru(NO)Cl. He determined that the Ru−η^2-NO linkage is unsymmetrical (Figure 5)[13] and that this isomer lies 1.23 eV (28.4 kcal/mol) in energy above the ground state.[14] The DFT calculations revealed a HOMO−4 orbital that involves efficient π bonding between the Ru d_{xz} orbital and the η^2-NO π^* orbital (if the *xz* plane is defined as the Ru−η^2-NO plane).

In addition, however, the HOMO−3 orbital revealed a preferential π-bonding interaction between the Ru d_{yz} orbital with the N end of the NO π^* orbital, leading to the rather unsymmetrical Ru(η^2-NO) geometry.

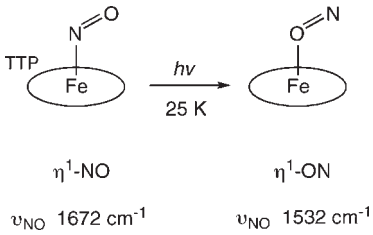

Figure 6. Light-induced generation of the metastable isonitrosyl linkage isomer of (TTP)Fe(NO) as a KBr pellet.[15]

Importantly, the observed downshifts (by 3−5 cm^{-1}) in some porphyrin skeletal absorption bands upon photolysis of these {RuNO}^{6} porphyrins indicated a reduction of the π-acid character of the NO ligand in the metastable states.[12] We will return later to this variation in the π acidity of the NO ligand.

Iron Porphyrins. Given our success at generating metastable nitrosyl linkage isomers of {RuNO}^{6} porphyrins, our RA−C−B team explored the possibility that such linkage isomers may exist for biologically relevant FeNO systems. We focused initially on the known {FeNO}^{7} five-coordinate (por)Fe(NO) class of compounds for proof of concept because (i) many of these were known to be thermally stable in the ground state and (ii) these compounds could be obtained in elementally pure form.[1]

Photolysis of the (TTP)Fe(NO) compound (TTP = tetratolylporphyrinato dianion) as a KBr pellet (350 < λ < 550 nm; Xe lamp) at 25 K for 5−10 min results in the generation of a new band in the IR spectra assigned to the metastable η^1-O isonitrosyl derivative (Figure 6).[15] Isotopic labeling with ^{15}NO and $^{15}N^{18}O$ confirmed that the new band was due to ν(NO).

Similar IR spectral shifts were observed with (OEP)Fe(NO), although in this latter case, a second photoproduct was also generated. As with the ruthenium case, these new bands generated upon photolysis disappeared upon warming and the original ν(NO) bands due to the ground-state compounds were restored, although the yields of the photoproducts [2−3% for (TTP)Fe(NO) and 6−10% for (OEP)Fe(NO)] were higher than those obtained from photolysis of the six-coordinate ruthenium compounds described earlier. Additional evidence for generation of the metastable isonitrosyl (TTP)Fe(η^1-ON) was provided by DFT calculations on the model (porphine)Fe(NO) compound.[15] Calculations on the ground-state (porphine)Fe(NO) compound reproduced the structural distortions of the N_4Fe(NO) core that had been demonstrated crystallographically by Scheidt and co-workers for (OEP)Fe(NO).[16,17] For example, our DFT calculations showed that the Fe−N(O) vector was tilted toward the O atom by 7.8° from the *z* axis defined by the normal to the porphyrin N_4 plane [a similar tilt of 6−8° was determined experimentally for (OEP)Fe(NO)[16,17]], and the NO group was staggered with respect to the Fe−N(por) bonds.

(13) Ghosh, A. *Acc. Chem. Res.* **2005**, *38*, 943–954.
(14) Wondimagegn, T.; Ghosh, A. *J. Am. Chem. Soc.* **2001**, *123*, 5680–5683.
(15) Cheng, L.; Novozhilova, I.; Kim, C.; Kovalevsky, A.; Bagley, K. A.; Coppens, P.; Richter-Addo, G. B. *J. Am. Chem. Soc.* **2000**, *122*, 7142–7143.
(16) Ellison, M. K.; Scheidt, W. R. *J. Am. Chem. Soc.* **1997**, *119*, 7404–7405.
(17) Scheidt, W. R.; Duval, H. F.; Neal, T. J.; Ellison, M. K. *J. Am. Chem. Soc.* **2000**, *122*, 4651–4659 and references cited therein.

Table 2. Selected Calculated Geometrical Parameters (in Å and deg) for the Ground-State and Isonitrosyl Isomers of the Unsubstituted (porphine)Fe(NO) Compound[15]

	(P′)Fe(NO)	(P′)Fe(ON)
Fe−NO	1.666	
Fe−ON		1.797
N−O	1.169	1.163
Fe−N−O	142.5	
Fe−O−N		141.0
Fe−NO/−ON tilt	7.8	10.8
Fe−N(por)	1.971	1.949
	1.946	1.938
ΔFe (por-N_4)	0.224	0.171

Further, the pair of Fe−N(por) bonds closest to the bent FeNO moiety was calculated to be ~0.025 Å *shorter* than the other pair directed away from the bent FeNO group.

The DFT calculations revealed the existence of the metastable (porphine)Fe(η^1-ON) linkage isomer that was 1.59 eV (36.7 kcal/mol) in energy above the ground-state nitrosyl.[15] The calculated geometries for the ground-state (porphine)Fe(NO) and metastable (porphine)Fe(η^1-ON) linkage isomers are shown in Figure 7, and selected structural data are collected in Table 2.

As seen in Figure 7, the calculated structure of the metastable (porphine)Fe(η^1-ON) isonitrosyl (bottom of the figure) closely resembles that of the ground-state compound (top of the figure).[15] Thus, the axial Fe−O(N) tilt and the nonequivalence of the two pairs of Fe−N(por) bond distances are properties of the isonitrosyl as well. The calculated axial Fe−ON tilt of 10.8° is larger than the 7.8° determined for the nitrosyl, and the apical displacement of the Fe atom from the porphine N_4 plane is smaller. The relevance of the latter structural feature to the π-acid property of the isonitrosyl ligand may be related to an intrinsic reduction in the π acidity of NO when the FeNO moiety converts to the FeON isonitrosyl (see later).

Related DFT calculations (PW91 exchange-correlation functional) on (por)Fe(NO) and other nitrosyl metalloporphyrins of cobalt, manganese, and rhodium have been reported by Ghosh and co-workers, who also explored the existence and stabilities of isonitrosyl derivatives.[14,18] Ghosh[13,18] and Coppens[19] have provided additional insight into the axial Fe−N/O tilts in the ground-state (porphine)-Fe(NO) and metastable (porphine)Fe(η^1-ON) compounds, respectively. In both cases, increased interaction between the NO π^* orbital and a "tilted" Fe d_{z^2} orbital is favored when the axial Fe−N/O vector is tilted. Such "tilting" of the Fe d_{z^2} orbital has been shown to be particularly pronounced for related six-coordinate iron nitrosylporphyrins.[20]

Our RA−C−B team then explored the possibility that metastable isonitrosyl compounds could be generated in six-coordinate $\{FeNO\}^6$ systems. For this, we chose to use Yoshimura's nitrosylnitro compound (TPP)Fe-(NO)(NO_2) (TPP = tetraphenylporphyrinato dianion) that could be obtained in an elementally pure state.[21] The ground-state structure of (TPP)Fe(NO)(NO_2) possesses mutually trans η^1-NO and η^1-NO_2 ligands, as was initially demonstrated by spectroscopy by Yoshimura[21] and Settin and Fanning,[22] and later by the crystallographic characterization of several (por)Fe(NO)(NO_2) derivatives by Scheidt and co-workers.[23] The crystal structure of the target compound (TPP)Fe(NO)(NO_2) unfortunately suffered from severe disorder, thus limiting the usefulness of the metrical data. We note, however, that, although the crystal structures of most of the crystal forms of (TpivPP)Fe(NO)(NO_2) (TpivPP = picket-fence porphyrinato dianion) display linear FeNO geometries, that of (T(*p*-OMe)PP)Fe(NO)(NO_2) displays an Fe−N−O angle of 160°.[23]

To further characterize these (por)Fe(NO)(NO_2) compounds, we performed DFT calculations on the parent (porphine)Fe(NO)(NO_2) model compound.[24,25] The calculations confirmed that the η^1-NO nitrosyl and η^1-NO_2 nitro binding modes were present in the ground-state (GS) structure. The presence of a bent FeNO moiety in this formally $\{FeNO\}^6$ compound was evident; the two FeNO angles of 156.4° ($GS_{\parallel}$) and 159.8° ($GS_{\perp}$) corresponded to the two GS conformations with mutually parallel ($\parallel$) and perpendicular ($\perp$) axial FeNO and $FeNO_2$ planes, respectively. Importantly, the calculated electron localization function (ELF) revealed a noncylindrical electron-pairing region on the nitrosyl N atom (Figure 8). This result demonstrated, for the first time, a "ferrous $\{FeNO\}^7$-like" electron-pair localization in a formally "ferric" $\{FeNO\}^6$ porphyrin system.

Photolysis of (TPP)Fe(NO)(NO_2) as a KBr pellet ($330 < \lambda < 500$ nm; Xe lamp) at low temperature resulted in several IR spectral shifts that could be rationalized by transformations to generate both nitrosyl and nitrite linkage isomers shown in Figure 9.

Irradiation of this compound at 11 K for 10 min produces shifts in the IR spectrum consistent with transformation of the nitrosyl to an isonitrosyl Fe(η^1-ON) group [ν(NO) 1699 cm^{-1}] as well as an Fe(NO_2)-to-Fe(ONO) conversion. The identities of the bands were confirmed by ^{15}N labeling. The 1699 cm^{-1} band was observable only at very low temperatures (e.g., temperatures ≤ 50 K); warming the sample to 200 K results in the disappearance of this band. The new bands due to the FeONO group were, however, retained even at 200 K. We were unable to use the IR data obtained at 11 K to distinguish between a mixture of the singly isomerized species (i.e., MSa + MSb) and the doubly isomerized species (MSc). Thus, we employed DFT calculations to help provide insight into the existence and stabilities of these single and double linkage isomers shown in Figure 9. In all, 10 optimized structures were determined: 2 for the ground state ($GS_{\parallel}$ and $GS_{\perp}$), 3 for the nitrosylnitrito ($MSa_{\parallel}$, $MSa_{\perp}$, and MSa_L), 2 for the isonitrosylnitro ($MSb_{\parallel}$ and $MSb_{\perp}$), and 3 for the isonitrosylnitrito double-linkage isomers ($MSc_{\parallel}$, $MSc_{\perp}$, and MSc_L). The "L"

(18) Ghosh, A.; Wondimagegn, T. *J. Am. Chem. Soc.* **2000**, *122*, 8101–8102.
(19) Coppens, P.; Novozhilova, I.; Kovalevsky, A. *Chem. Rev.* **2002**, *102*, 861–883.
(20) Praneeth, V. K. K.; Nather, C.; Peters, G.; Lehnert, N. *Inorg. Chem.* **2006**, *45*, 2795–2811.
(21) Yoshimura, T. *Inorg. Chim. Acta* **1984**, *83*, 17–21.
(22) Settin, M. F.; Fanning, J. C. *Inorg. Chem.* **1988**, *27*, 1431–1435.
(23) Ellison, M. K.; Schulz, C. E.; Scheidt, W. R. *Inorg. Chem.* **1999**, *38*, 100–108.
(24) Novozhilova, I. V.; Coppens, P.; Lee, J.; Richter-Addo, G. B.; Bagley, K. A. *J. Am. Chem. Soc.* **2006**, *128*, 2093–2104.
(25) Lee, J.; Kovalevsky, A. Y.; Novozhilova, I. V.; Bagley, K. A.; Coppens, P.; Richter-Addo, G. B. *J. Am. Chem. Soc.* **2004**, *126*, 7180–7181.

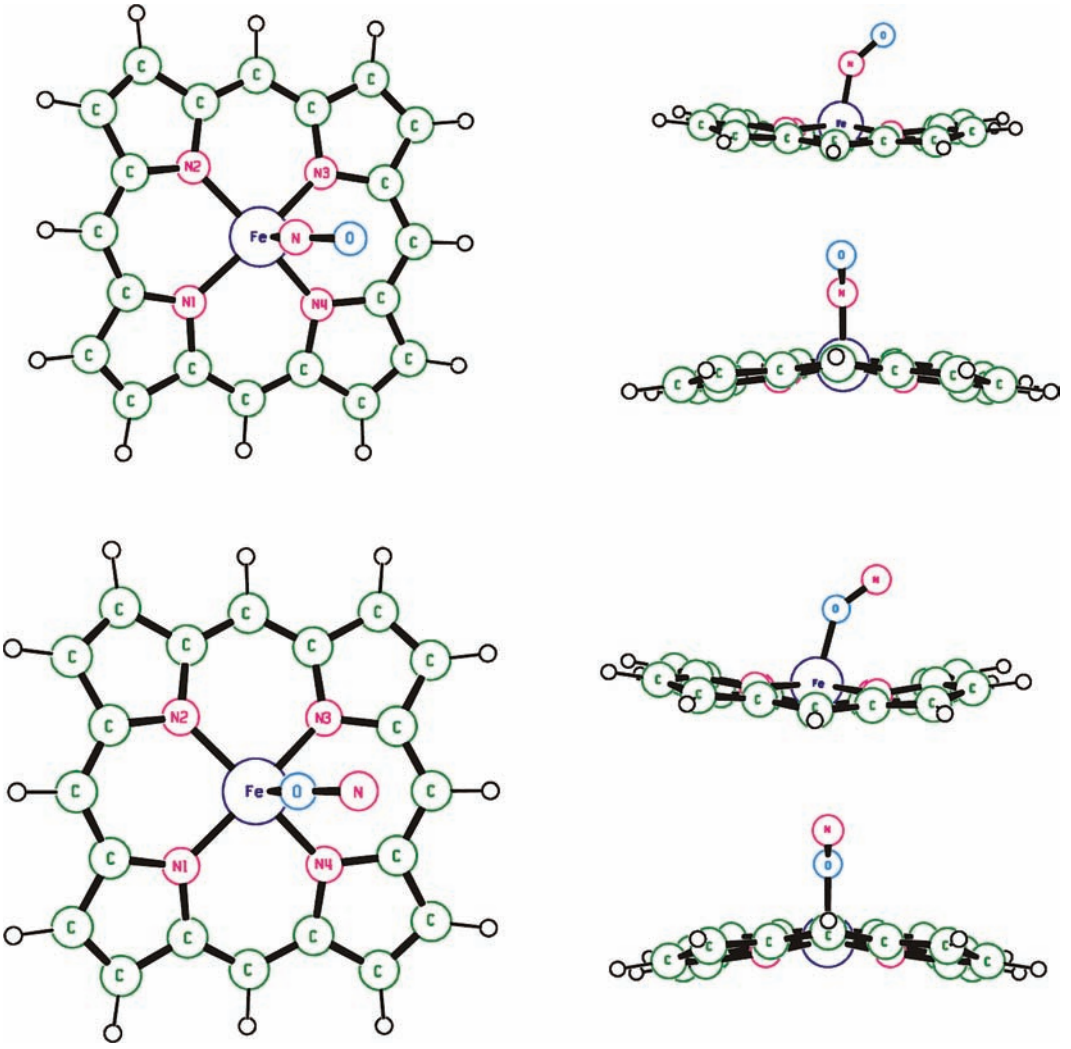

Figure 7. Calculated geometries of the ground-state (porphine)Fe(NO) (top) and its metastable isonitrosyl derivative (bottom) viewed from three different directions (reproduced in part from ref 15). Valence shells of the H, C, N, and O atoms were described by a double-ζ STO basis set extended with a polarization function, whereas the 3s, 3p, and 3d shells on the Fe atom were described by a triple-ζ STO basis set (ADF program package).

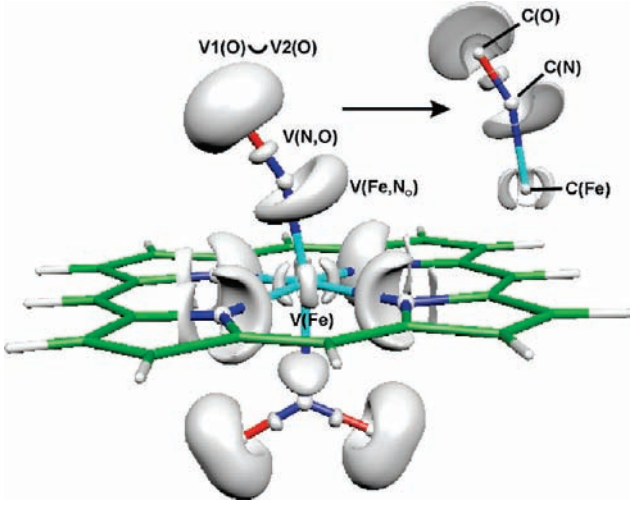

Figure 8. ELF of the ground-state (porphine)Fe(NO)(NO_2), with a plotted isosurface value of 0.8. Reproduced with permission from ref 24. Copyright 2006 The American Chemical Society.

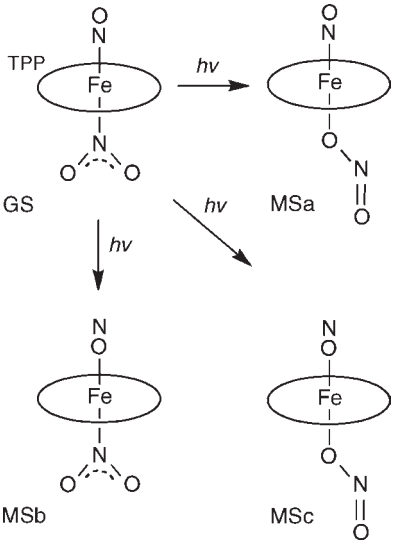

Figure 9. Light-induced transformations upon irradiation of (TPP)Fe(NO)(NO_2) as a KBr pellet at low temperatures.[24]

notation symbolizes those conformations with linear FeNO and FeON moieties; interestingly, these were calculated to be *higher* in energy than their bent counterparts in these formally $\{FeNO\}^6$ systems. The calculated

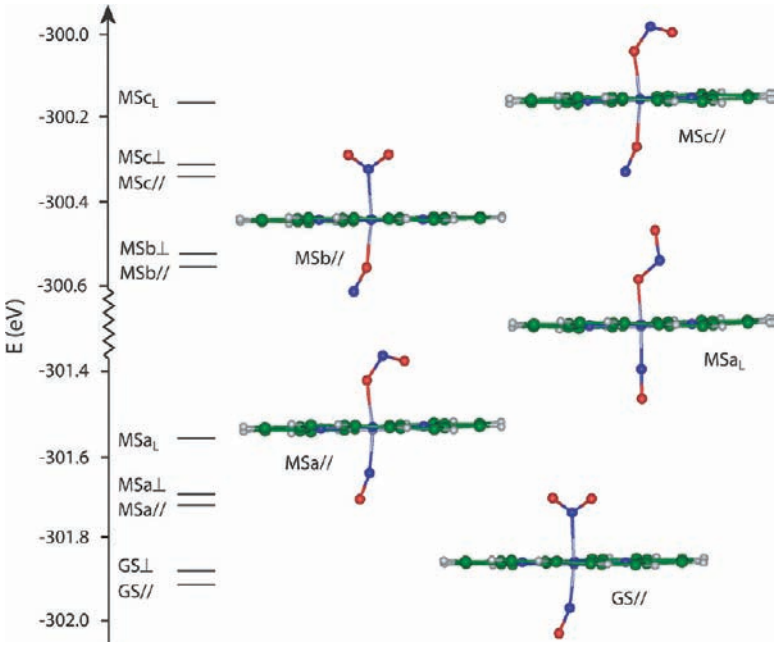

Figure 10. Calculated energies and representative structures for the linkage isomers of (porphine)Fe(NO)(NO_2). ∥ = axial ligand planes are coplanar; ⊥ = axial ligand planes are mutually perpendicular; MSa_L and MSc_L are the isomers displaying linear FeNO and FeON groups, respectively. Reproduced from ref 25. Copyright 2004 The American Chemical Society.

energies and sketches of representative examples of these linkage isomers are shown in Figure 10. The energies increase in the order GS ≪ nitrito (MSa) < isonitrosyl (MSb) < nitritoisonitrosyl (MSc). The double-linkage isomer MSc_L was determined to be the least stable, with an energy of 1.73 eV (40 kcal/mol) above the ground-state isomer $GS_{\|}$.[24]

The Fe−ON bonds in the isonitrosyl isomers (with calculated Mayer bond orders of 0.5−0.6) are longer than the Fe−NO bonds in the nitrosyl isomers (with calculated Mayer bond orders of 0.9−1.0). We attributed this feature to reduced back-donation into the antibonding π^* orbital in the Fe(η^1-ON) isonitrosyls. This analysis was consistent with the calculated smaller iron apical displacement out of the porphyrin N_4 plane in the isonitrosyls relative to that determined for the nitrosyls. Indeed, examination of the relevant molecular orbitals revealed that the shortening of the Fe−N(por) bonds in the isonitrosyls (when compared with the nitrosyls) was due to the increased π overlap in the Fe−N(por) bonds that accompanied the decrease in back-bonding to the axial isonitrosyl group.

The results of time-dependent DFT calculations confirmed that both the nitrosyl-to-isonitrosyl and nitro-to-nitrito isomerizations could be induced by 300−500 nm light. Indeed, Ford and co-workers had previously shown that flash photolysis of (TPP)Fe(NO)(NO_2) in a toluene solution at 298 K resulted in competitive dissociation of the axial NO and NO_2 ligands.[26] In our photolysis experiments with (TPP)Fe(NO)(NO_2) as a KBr pellet at low temperatures, however, both NO and NO_2 ligands were retained at the metal center in this medium.

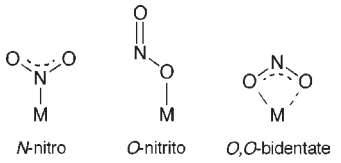

Figure 11. Nitrite binding modes to monometallic centers.

Nitrite Linkage Isomers

The nitrite anion (NO_2^-; pK_a 3.2 at 20 °C)[27] displays several coordination modes in its metal complexes.[28] Of relevance to this Forum Article are the three binding modes shown in Figure 11. We have already considered the nitro (metal−NO_2) and nitrito (metal−ONO) forms in the previous section. The nitrite O,O′-bidendate binding mode has been determined crystallographically for the nitrite adducts of the copper-containing nitrite reductase (NiR) from *Alcaligenes xylosoxidans* (the His313Gly mutant),[29] the soil bacterium *Achromobacter cycloclastes*,[8] and in synthetic copper complexes.[30] However, this O,O′-bidentate mode has not been determined for any metalloporphyrin or heme protein to date and, hence, will not be considered further.

Model Complexes. Our interest in nitrite coordination modes in heme models and heme proteins was to a large degree inspired by the evidence that we obtained for low-energy differences between the nitro Fe−NO_2 and nitrito Fe−ONO geometries during our photoinduced linkage isomerization experiments discussed above.[24,25] In particular, the calculated (and rather small) energy difference

(26) Lim, M. D.; Lorkovic, I. M.; Wedeking, K.; Zanella, A. W.; Works, C. F.; Massick, S. M.; Ford, P. C. *J. Am. Chem. Soc.* **2002**, *124*, 9737–9743.

(27) Braida, W.; Ong, S. K. *Water, Air, Soil Pollut.* **2000**, *118*, 13–26.

(28) Hitchman, M. A.; Rowbottom, G. L. *Coord. Chem. Rev.* **1982**, *42*, 55–132.

(29) Barrett, M. L.; Harris, R. L.; Antonyuk, S.; Hough, M. A.; Ellis, M. J.; Sawers, G.; Eady, R. R.; Hasnain, S. S. *Biochemistry* **2004**, *43*, 16311–16319.

(30) Lehnert, N.; Cornelissen, U.; Neese, F.; Ono, T.; Noguchi, Y.; Okamoto, K.-i.; Fujisawa, K. *Inorg. Chem.* **2007**, *46*, 3916–3933.

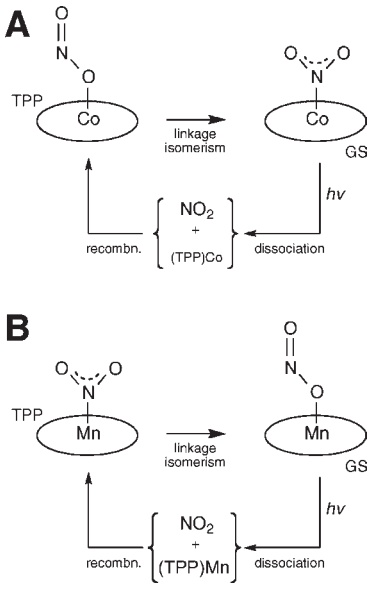

Figure 12. Proposed mechanisms for the linkage isomerization reactions after photolysis of the ground-state nitro (TPP)Co(NO_2) (A) and nitrito (TPP)Mn(ONO) (B) compounds.

of 4.3 kcal/mol between the $GS_{\|}$ and $MSa_{\|}$ isomers of (porphine)Fe(NO)(NO_2) raised our interest in examining the factors that could determine the coordination geometry of nitrite in its metalloporphyrin complexes. The crystal structures of synthetic iron porphyrin nitrite complexes display, regardless of the iron oxidation state, the nitro N-binding mode.[31−33] The only exception is that for the $[(TpivPP)Fe(NO)(NO_2)]^-$ anion, which exhibits a 40:60 disorder of the $FeNO_2$:FeONO binding modes in the same crystal.[34] It is reasonable to assume that the "distal pocket" provided by the −NH groups of the picket-fence porphyrin probably assists in the stabilization of the FeONO isomer in this complex anion.

The nitro binding mode prevails in the case of cobalt porphyrin nitrite complexes as well.[31,35,36] Demonstration of this prevalent N-binding mode can be obtained from the results of laser flash photolysis experiments performed on the five-coordinate (TPP)Co(NO_2) (Figure 12A).[37] Photolysis of this compound in benzene resulted in the formation of $(TPP)Co^{II}$ (determined spectroscopically) via photodissociation of the NO_2 ligand. The photodissociated NO_2 ligand then recombined with $(TPP)Co^{II}$ to give initially the metastable (TPP)Co(ONO) compound; a nitrito-to-nitro isomerization occurs to regenerate the thermally stable nitro (TPP)Co(NO_2) compound.

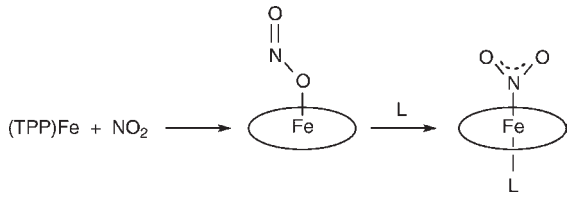

Figure 13. Reaction of nitrogen dioxide with sublimed layers of (TPP)Fe to give initially (TPP)Fe(ONO), followed by exogenous ligand-induced isomerization to the nitro isomer.

In contrast, the nitrite ligand is found to adopt a stable nitrito O-binding mode in the (TPP)Mn(ONO) compound.[38] Indeed, and in what appears to directly contrast the cobalt case just described, flash photolysis of the (TPP)Mn(ONO) complex in toluene results in the formation of $(TPP)Mn^{II}$ (determined spectroscopically) via dissociation of the NO_2 ligand; recombination produces the intermediate nitro complex (TPP)Mn(NO_2), which then isomerizes to the stable nitrito species (TPP)Mn(ONO) (Figure 12B).[39] The stable nitrito O-binding mode is also the only one observed to date in the crystal structures of the nitrite adducts of synthetic metalloporphyrins of ruthenium[40−43] and osmium.[44]

Such O binding of nitrite to iron porphyrins has been demonstrated spectroscopically by Ford and co-workers during the low-temperature reactions of NO_2 with sublimed layers of the four-coordinate (por)Fe compounds (por = TPP, TTP).[45] The reaction employing the TPP macrocycle is illustrated in Figure 13. In these reactions, the initially generated five-coordinate nitrito (por)Fe(ONO) compounds react further with the sixth ligands (L = NO, NH_3) to give the six-coordinate (por)Fe(ONO)(L) intermediates that isomerize upon warming to their more stable nitro isomers.[46−48] DFT calculations on the model five-coordinate (porphine)Fe(nitrite) compound (B3LYP functional; LACVP* basis set) predicted near-identical energies for the experimentally observed nitrito and the not-yet-observed nitro isomers.[46]

An earlier DFT calculation (B3LYP functional) on the model compound (porphine)Fe(NO_2)(NH_3) revealed a thermodynamic preference for the nitro binding mode in the ferric form by over 10 kcal/mol.[49] Related DFT calculations (UBP86 functional) on the six-coordinate

(31) Wyllie, G. R. A.; Scheidt, W. R. *Chem. Rev.* **2002**, *102*, 1067–1089.
(32) Nasri, H.; Ellison, M. K.; Shang, M.; Schultz, C. E.; Scheidt, W. R. *Inorg. Chem.* **2004**, *43*, 2932–2942.
(33) Cheng, L.; Powell, D. R.; Khan, M. A.; Richter-Addo, G. B. *Chem. Commun.* **2000**, 2301–2302.
(34) Nasri, H.; Ellison, M. K.; Chen, S.; Huynh, B. H.; Scheidt, W. R. *J. Am. Chem. Soc.* **1997**, *119*, 6274–6283.
(35) Adachi, H.; Suzuki, H.; Miyazaki, Y.; Iimura, Y.; Hoshino, M. *Inorg. Chem.* **2002**, *41*, 2518–2524.
(36) Goodwin, J.; Kurtikyan, T.; Standard, J.; Walsh, R.; Zheng, B.; Parmley, D.; Howard, J.; Green, S.; Mardyukov, A.; Przybla, D. E. *Inorg. Chem.* **2005**, *44*, 2215–2223.
(37) Seki, H.; Okada, K.; Iimura, Y.; Hoshino, M. *J. Phys. Chem. A* **1997**, *101*, 8174–8178.
(38) Suslick, K. S.; Watson, R. A. *Inorg. Chem.* **1991**, *30*, 912–919.
(39) Hoshino, M.; Nagashima, Y.; Seki, H.; Leo, M. D.; Ford, P. C. *Inorg. Chem.* **1998**, *37*, 2464–2469.
(40) Kadish, K. M.; Adamian, V. A.; Caemelbecke, E. V.; Tan, Z.; Tagliatesta, P.; Bianco, P.; Boschi, T.; Yi, G.-B.; Khan, M. A.; Richter-Addo, G. B. *Inorg. Chem.* **1996**, *35*, 1343–1348.
(41) Miranda, K. M.; Bu, X.; Lorkovic, I.; Ford, P. C. *Inorg. Chem.* **1997**, *36*, 4838–4848.
(42) Bohle, D. S.; Hung, C.-H.; Smith, B. D. *Inorg. Chem.* **1998**, *37*, 5798–5806.
(43) Lim, M. H.; Lippard, S. J. *Inorg. Chem.* **2004**, *43*, 6366–6370.
(44) Leal, F. A.; Lorkovic, I. M.; Ford, P. C.; Lee, J.; Chen, L.; Torres, L.; Khan, M. A.; Richter-Addo, G. B. *Can. J. Chem.* **2003**, *81*, 872–881.
(45) Heinecke, J.; Ford, P. C. *Coord. Chem. Rev.* **2010**, *254*, 235–247.
(46) Kurtikyan, T. S.; Hovhannisyan, A. A.; Hakobyan, M. E.; Patterson, J. C.; Iretskii, A.; Ford, P. C. *J. Am. Chem. Soc.* **2007**, *129*, 3576–3585.
(47) Kurtikyan, T. S.; Ford, P. C. *Angew. Chem., Int. Ed.* **2006**, *45*, 492–496.
(48) Kurtikyan, T. S.; Hovhannisyan, A. A.; Gulyan, G. M.; Ford, P. C. *Inorg. Chem.* **2007**, *46*, 7024–7031.
(49) Einsle, O.; Messerschmidt, A.; Huber, R.; Kroneck, P. M. H.; Neese, F. *J. Am. Chem. Soc.* **2002**, *124*, 11737–11745.

(porphine)Fe(NO_2)(ImdH) showed a preference, by 4.5 kcal/mol, for the nitro binding mode (6 kcal/mol in the ferrous form).[50] Similar results were obtained in a recent study, and the results show a preference, by 5−10 kcal/mol (depending on the basis sets used), for the nitro binding modes.[51]

Heme Proteins. The heme−nitrite interaction in proteins has a rather long history. In bacterial denitrification, the NiR enzymes converts nitrite to NO.[52−56] The initial binding of nitrite to the heme iron in the active site is generally regarded as a requirement for the NiR activity of these proteins (eq 1).

$$NO_2^- + 2H^+ + 1e^- \rightarrow NO + H_2O \qquad (1)$$

Nitrite has also been used for many generations in the curing of meat.[57−60] In addition to its antimicrobial and antioxidant activity, nitrite restores the pink color of meat by formation of the myoglobin (Mb) heme−NO pigment.[61] However, nitrite can also be harmful to mammals because it can oxidize ferrous hemoglobin (Hb) and increase the in vivo levels of ferric Hb to result in the blood disorder methemoglobinemia.[62,63]

The relevance of nitrite to mammalian physiology is currently being actively studied, and a biannual international conference on The Role of Nitrite in Physiology, Pathophysiology and Therapeutics has been established.[64,65] It is now known that several mammalian metalloenzymes will reduce nitrite to NO.[66,67] The demonstration by Hendgen-Cotta et al. that nitrite protects against myocardial infarction in $Mb^{+/+}$ mice but not in $Mb^{-/-}$ knockout mice implicates Mb as an in vivo NiR.[68] The chemistry of the heme−nitrite interactions relevant to mammalian physiology has been recently reviewed.[45]

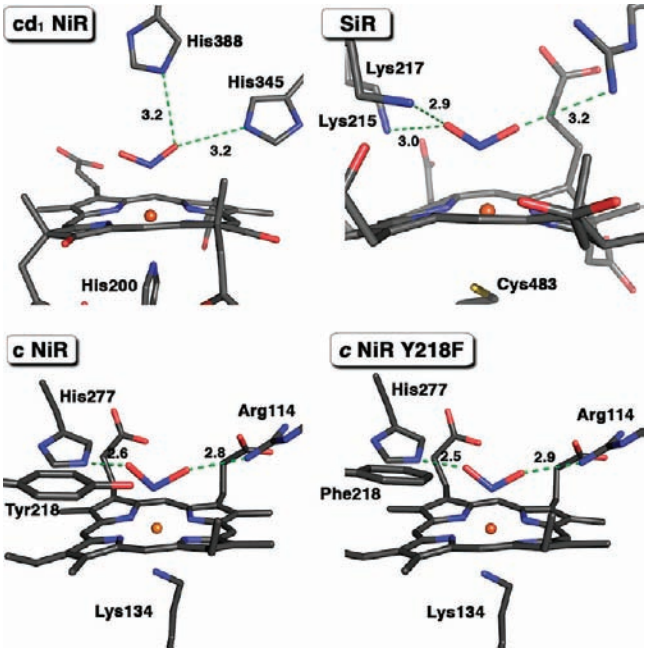

Figure 14. Heme active sites of the N-bound nitrite adducts of cytochrome cd_1 NiR from *P. pantotrophus* (top left; 1.8 Å resolution; PDB access code 1AAQ), the sulfite reductase hemoprotein from *E. coli* (top right; 2.1 Å resolution; PDB access code 3GEO), cytochrome *c* NiR from *W. succinogenes* (bottom left; 1.6 Å resolution), and its Y218F mutant (bottom right; 1.75 Å resolution; PDB access code 3BNH).

Despite the generally acknowledged medical importance of nitrite interactions with the mammalian proteins Mb and Hb, we were surprised to find out that there was no crystal structural data for either the Mb−nitrite or Hb−nitrite adducts. The reported crystal structures for the nitrite adducts of the cytochrome cd_1 NiR from *Paraccocus pantotrophus*,[69] the sulfite reductase hemoprotein from *Escherichia coli*,[70] and the cytochrome *c* NiR from *Wolinella succinogenes*[49] all revealed the N binding of nitrite to the active site iron centers (i.e., nitro binding mode), as shown in Figure 14. In all cases, the bound nitrite ligand engaged in more than one H-bonding interaction with distal pocket residues. Recently, the crystal structure of the nitrite adduct of the cytochrome *c* NiR Y218F mutant was reported; the bound nitrite retained its N-binding mode in this mutant that has a conserved Tyr residue mutated to Phe (Figure 14, bottom right).[71]

(50) Silaghi-Dumitrescu, R. *Inorg. Chem.* **2004**, *43*, 3715–3718.
(51) Perissinotti, L. L.; Marti, M. A.; Doctorovich, F.; Luque, F. J.; Estrin, D. A. *Biochemistry* **2008**, *47*, 9793–9802.
(52) Averill, B. A. *Chem. Rev.* **1996**, *96*, 2951–2964.
(53) Eady, R. R.; Hasnain, S. S. In *Comprehensive Coordination Chemistry II*; Que, L., Jr., Tolman, W. B., Eds.; Elsevier: San Diego, CA, 2004; Vol. *8*, pp 759−786.
(54) Hollocher, T. C. In *Nitric Oxide. Principles and Applications*; Lancaster, J., Ed.; Academic Press: San Diego, CA, 1996; pp 289−344.
(55) Hollocher, T. C.; Hibbs, J. B., Jr. In *Methods in Nitric Oxide Research*; Feelish, M., Stamler, J. S., Eds.; John Wiley and Sons: Chichester, U.K., 1996; pp 119−146.
(56) Tavares, P.; Pereira, A. S.; Moura, J. J. G. *J. Inorg. Biochem.* **2006**, *100*, 2087–2100.
(57) Skibsted, L. H. In *The Chemistry of Muscle-Based Foods*; Johnson, D. E., Knight, M. K., Ledward, D. A., Eds.; Royal Society of Chemistry: Cambridge, U.K., 1992; pp 266−286.
(58) Livingston, D. J.; Brown, W. D. *Food Technol.* **1981**, May Issue, 244–252 and references cited therein.
(59) Killday, K. B.; Tempesta, M. S.; Bailey, M. E.; Metral, C. J. *J. Agric. Food Chem.* **1988**, *36*, 909–914.
(60) Bruun-Jensen, L.; Skibsted, L. H. *Meat Sci.* **1996**, *44*, 145–149.
(61) Møller, J. K. S.; Skibsted, L. H. *Chem. Rev.* **2002**, *102*, 1167–1178.
(62) Percy, M. J.; McFerran, N. V.; Lappin, T. R. J. *Blood Rev.* **2005**, *19*, 61–68.
(63) Chui, J. S.; Poon, W. T.; Chan, K. C.; Chan, A. Y.; Buckley, T. A. *Anaesthesia* **2005**, *60*, 496–500.
(64) Gladwin, M. T.; Schechter, A. N.; Kim-Shapiro, D. B.; Patel, R. P.; Hogg, N.; Shiva, S.; Cannon, R. O., III; Kelm, M.; Wink, D. A.; Espey, M. G.; Oldfield, E. H.; Pluta, R. M.; Freeman, B. A.; Lancaster, J. R., Jr.; Feelisch, M.; Lundberg, J. O. *Nat. Chem. Biol.* **2005**, *1*, 308–314 and references cited therein [Erratum: 2006, 2 (2), 110.].
(65) Lundberg, J. O.; Gladwin, M. T.; Ahluwalia, A.; Benjamin, N.; Bryan, N. S.; Butler, A.; Cabrales, P.; Fago, A.; Feelisch, M.; Ford, P. C.; Freeman, B. A.; Frenneaux, M.; Friedman, J.; Kelm, M.; Kevil, C. G.; Kim-Shapiro, D. B.; Kozlov, A. V.; Lancaster, J. R.; Lefer, D. J.; McColl, K.; McCurry, K.; Patel, R. P.; Petersson, J.; Rassaf, T.; Reutov, V. P.; Richter-Addo, G. B.; Schechter, A.; Shiva, S.; Tsuchiya, K.; van Faassen, E. E.; Webb, A. J.; Zuckerbraun, B. S.; Zweier, J. L.; Weitzberg, E. *Nat. Chem. Biol.* **2009**, *5*, 865–869.
(66) van Faassen, E. E.; Babrami, S.; Feelisch, M.; Hogg, N.; Kelm, M.; Kim-Shapiro, D. B.; Kozlov, A. V.; Li, H. T.; Lundberg, J. O.; Mason, R.; Nohl, H.; Rassaf, T.; Samouilov, A.; Slama-Schwok, A.; Shiva, S.; Vanin, A. F.; Weitzberg, E.; Zweier, J.; Gladwin, M. T. *Med. Res. Rev.* **2009**, *29*, 683–741.
(67) Feelisch, M.; Fernandez, B. O.; Bryan, N. S.; Garcia-Saura, M. F.; Bauer, S.; Whitlock, D. R.; Ford, P. C.; Janero, D. R.; Rodriguez, J.; Ashrafian, H. *J. Biol. Chem.* **2008**, *283*, 33927–33934.
(68) Hendgen-Cotta, U. B.; Merx, M. W.; Shiva, S.; Schmitz, J.; Becher, S.; Klare, J. P.; Steinhoff, H. J.; Goedecke, A.; Schrader, J.; Gladwin, M. T.; Kelm, M.; Rassaf, T. *Proc. Natl. Acad. Sci. U.S.A.* **2008**, *105*, 10256–10261 [Erratum: p 12636].
(69) Williams, P. A.; Fulop, V.; Garman, E. F.; Saunders, N. F. W.; Ferguson, S. J.; Hajdu, J. *Nature* **1997**, *389*, 406–412.
(70) Crane, B. R.; Siegel, L. M.; Getzoff, E. D. *Biochemistry* **1997**, *36*, 12120–12137.
(71) Lukat, P.; Rudolf, M.; Stach, P.; Messerschmidt, A.; Kroneck, P. M. H.; Simon, J.; Einsle, O. *Biochemistry* **2008**, *47*, 2080–2086.

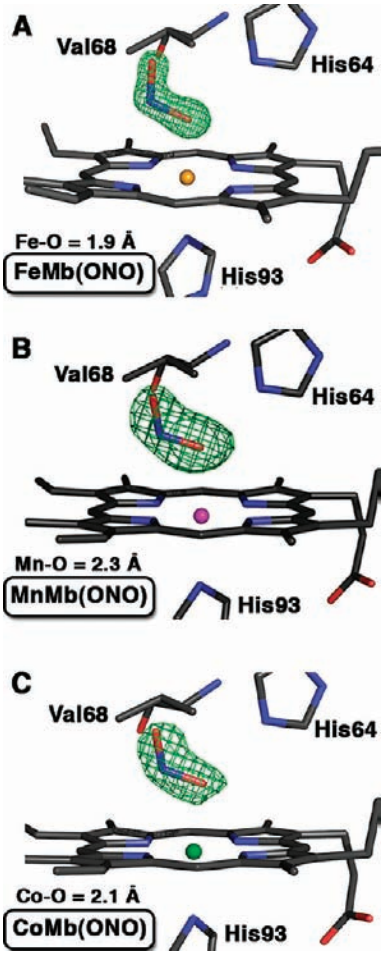

Figure 15. $F_o - F_c$ omit electron density maps (contoured at 3σ) and final models of the heme environments of the O-bound nitrite adducts of (A) wild-type horse heart ferric Mb (1.20 Å resolution; PDB access code 2FRF),[72] (B) Mn^{III}-substituted Mb (1.60 Å resolution; PDB access code 2O5O),[73] and (C) Co^{III}-substituted Mb (1.60 Å resolution; PDB access code 2O5S).[73]

We mentioned earlier that despite the importance of the Mb−nitrite and Hb−nitrite interactions, there were no reported crystal structures of these compounds. We were successful at crystallizing the nitrite adduct of ferric horse heart Mb and determining its crystal structure at 1.20 Å resolution (top of Figure 15).[72] The nitrite ligand in this formally Mb^{III}(ONO) complex binds to the ferric center through one of its O atoms, namely, in the nitrito O-binding mode. At the time, this was the first report of O binding of nitrite to any heme protein. The nitrito ligand was stabilized by H bonding to the distal His64 residue using its O1 atom. Importantly, the same Fe−ONO geometry was obtained regardless of whether the complex was generated by soaking crystals of preformed metMb with nitrite or by crystallizing preformed Mb−nitrite from solution. This suggested that the nitrito FeONO formation, with Fe in the d^5 electronic configuration, was the ground-state geometry. Various attempts to generate a ferrous Mb−nitrite complex for a crystal structural determination were unsuccessful. We thus proceeded to prepare and determine the structures

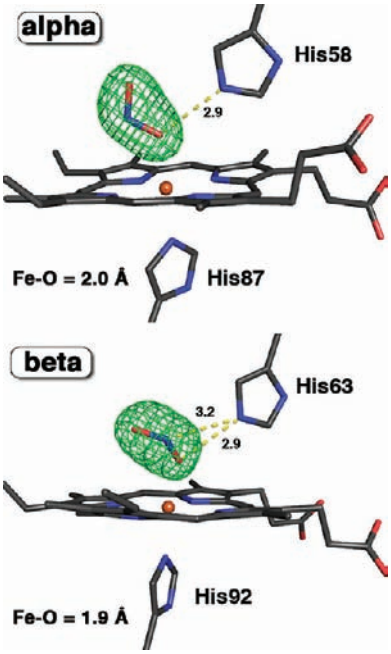

Figure 16. $F_o - F_c$ omit electron density maps (contoured at 3σ) and final models of the heme environments of the O-bound nitrite adduct of ferric human Hb (1.80 Å resolution; PDB access code 3D7O).[74]

of the related Mn^{III}-substituted (a d^4 system) and Co^{III}-substituted (a d^6 system) derivatives.

The 1.60 Å resolution crystal structure of the Mn^{III}-substituted Mb−nitrite complex is shown in the middle of Figure 15; the nitrite ligand is also O-bound in this derivative.[73] This is not too surprising because the nitrite adduct of the synthetic compound (TPP)Mn(ONO) reveals this stable O-binding mode.[38] What was surprising to us, however, was the retention of the O-binding mode of nitrite in the d^6 Co^{III}-substituted derivative (bottom of Figure 15).[73] We noted earlier that the crystal structures of all reported nitrite adducts of cobalt porphyrins displayed the N-binding mode of nitrite. This suggested to us that the distal His64 residue in Mb played a critical role in directing the nitrite ligand toward this O-binding mode in this d^6 cobalt(III) nitrite complex [formally valence isoelectronic with the iron(II) nitrite compound].

We then examined the nitrite binding mode(s) in the nitrite adduct of ferric human Hb. The heme sites of the nitrite adduct of the ferric Hb, as determined from the 1.80 Å crystal structure, are shown in Figure 16. As is evident in the figure, the nitrite ligand also displays the O-binding mode to the iron centers in both the α and β subunits.[74] However, the FeONO conformations were found to differ between these two subunits. The FeONO conformation was trans in the α subunit (Fe−O−N−O torsion angle of 174°) but deviated from trans toward a distorted cis-like conformation in the β subunit (Fe−O−N−O torsion angle of −91°). The limiting trans and cis conformations are shown in Figure 17.

Our observation of the previously "rare" O-binding mode of nitrite in both Mb and Hb led us to further

(72) Copeland, D. M.; Soares, A.; West, A. H.; Richter-Addo, G. B. *J. Inorg. Biochem.* **2006**, *100*, 1413–1425.

(73) Zahran, Z. N.; Chooback, L.; Copeland, D. M.; West, A. H.; Richter-Addo, G. B. *J. Inorg. Biochem.* **2008**, *102*, 216–233.

(74) Yi, J.; Safo, M. K.; Richter-Addo, G. B. *Biochemistry* **2008**, *47*, 8247–8249.

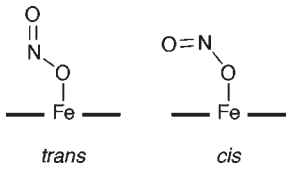

Figure 17. Sketches of the trans and cis FeONO conformations.

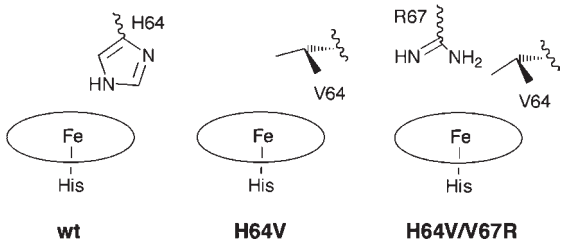

Figure 18. Sketches of the actives sites of wild-type Mb (left), the H64V mutant (middle), and the H64V/V67R double mutant (right).

examine the role of the distal His64 (Mb numbering) residue in the active sites of these proteins. We hypothesized that it was this single H-bonding residue that directed the nitrite ligand toward the O-binding mode. If this were the case, then removing this H-bonding residue should allow the nitrite ligand to adopt its more "common" N-binding mode, as observed in almost all ground-state synthetic models lacking distal pockets. For example, the H64V mutant of Mb would not have this distal H-bonding capacity, as sketched in the middle of Figure 18.

To test this hypothesis, we prepared the nitrite adduct of the H64V mutant of Mb, crystallized it, and solved its 1.95 Å resolution crystal structure. The heme site of this H64V Mb−nitrite compound is shown at the top of Figure 19.[75] The Fe−nitrite bond distance was unrestrained throughout the refinement, and the nitrite ligand was modeled in the N-binding mode at 65% occupancy. The lack of a distal His64 residue to stabilize the bound nitrite allows for a water channel to form from the exterior of the protein to contact the bound nitrite ligand. We speculate, based on the available data at this resolution, that the rather long Fe−NO_2 distance of 2.6 Å is probably due to a weak electrostatic interaction of the nitrite ligand with the ferric center within the hydrophobic pocket of this mutant.

Did the lack of a H-bonding residue in the distal pocket of Mb direct the nitrite ligand toward the N-binding mode? We further hypothesized that reintroduction of a H-bonding residue into the pocket, as would be extant in the H64V/V67R double mutant shown on the right side of Figure 18 (where Arg has replaced the non-H-bonding Val67 residue), would permit the nitrite to again adopt the O-binding mode.

The heme site of the nitrite adduct of Mb H64V/V67R is shown at the bottom of Figure 19.[75] In this structure, the nitrite ligand was modeled in the active site in the O-binding mode (as a distorted cis FeONO conformation) at 65% occupancy, and it H-bonds to a water molecule near the surface of the protein.

Clearly, it is evident that the single H-bonding residue in Mb, namely, the His64 residue, is important in determining

(75) Yi, J.; Heinecke, J.; Tan, H.; Ford, P. C.; Richter-Addo, G. B. *J. Am. Chem. Soc.* **2009**, *131*, 18119–18128.

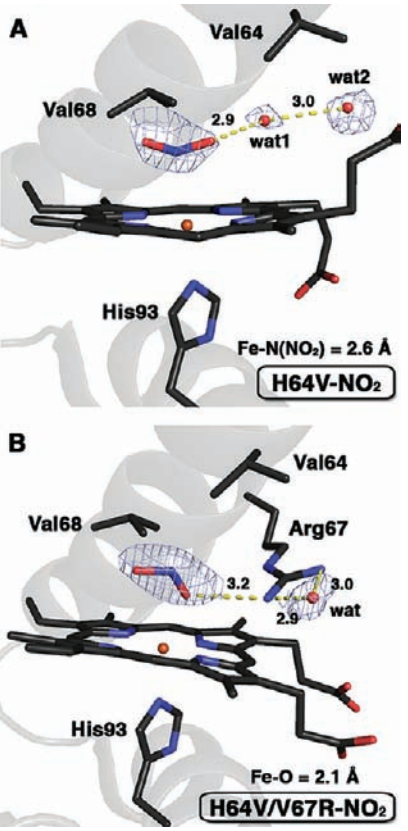

Figure 19. $F_o - F_c$ omit electron density maps (contoured at 3σ) and final models of the heme environments of (A) the N-bound nitrite adduct of the ferric Mb H64V mutant (1.95 Å resolution; PDB access code 3HEP) and (B) the O-bound nitrite adduct the ferric Mb H64V/V67R double mutant (2.0 Å resolution; PDB access code 3HEO).[75]

the binding conformation of the nitrite ligand in Mb (and probably in Hb as well). The effects of these mutations on the NiR activities of these mutants were explored; the rates follow the order wt > H64V/V67R ≫ H64V, suggesting a significant role of the distal pocket H-bonding residue in the reduction of nitrite to NO.[75] The classic nitrite N-binding mode has been used to help understand nitrite reduction in bacterial denitrifying enzymes (namely, a formal double protonation of a terminal O atom accompanies nitrite reduction). However, it has been calculated that the O-binding mode is also viable for nitrite reduction (a formal protonation of the O1 atom would result in the release of NO) for cytochrome cd_1[50] and for Hb.[51] Both of these pathways are shown schematically in Figure 20, and in the case of Hb, the involvement of the distal His residue as a proton donor is presumed.[51]

The crystallographic demonstration of both N binding (previous) and O binding (recent) of nitrite to heme proteins now raises new possibilities to study differential nitrite reduction by various heme proteins under different conditions. It should prove interesting to eventually determine which linkage isomers are operative under normal and abnormal physiological conditions.

Metal Hyponitrite Complexes

Hyponitrites can be considered as anionic derivatives of the NO dimer (Figure 21); hence, it is appropriate to provide a brief discussion of the NO dimer.

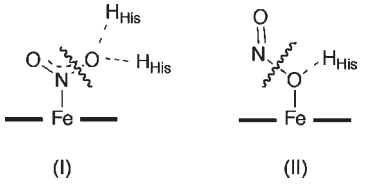

Figure 20. Probable protonation pathways involving the bound nitrite ligands to generate FeNO (left; I) and free NO (right, II).

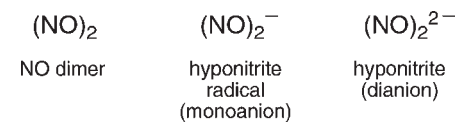

Figure 21. Redox congeners of the NO dimer.

NO dimer formation is enhanced at low temperature in condensed phases of NO[76] and by its location in hydrophobic environments such as those encountered in single-walled carbon nanotubes[77] and aromatic environments.[78] The neutral NO dimer, $(NO)_2$, consists of two NO moieties with a weak N−N bond with a binding energy of ∼2 kcal/mol.[78,79] The results of several experimental and computational studies of the neutral dimer $(NO)_2$ indicate that the ground-state *cis*-ONNO geometry is the most stable for this compound.[80] Fuster and co-workers have reexamined the bonding interactions between the NO moieties in the neutral dimer and mono- and dianionic redox partners using theoretical calculations.[79] They concluded that, although the *cis*-ONNO isomer was favored for the neutral species, the *trans*-ONNO geometry was favored for both the reduced monoanion $(NO)_2^-$, and dianion $(NO)_2^{2-}$ derivatives (the cis and trans forms of the dianion are sketched in Figure 22).

Further, they calculated that the N−N bonds became shorter in the order $(NO)_2 > (NO)_2^- > (NO)_2^{2-}$ in both the cis and trans geometries; these results reaffirmed the earlier and similar report by Snis and Panas.[81] Theoretical treatments[82−84] and IR experimental data[85] for the monoanionic hyponitrite radical have been reported. The increased strength of the ON−NO interaction in the anionic derivatives is consistent with the successful experimental isolation of several dianionic $(NO)_2^{2-}$ salts, termed hyponitrite salts, that contain formal N=N double bonds.

The reaction of alkali metals with NO generates alkali-metal hyponitrites. For example, the reaction of sodium with

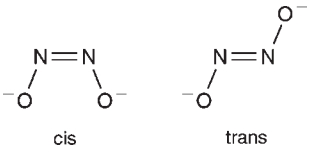

Figure 22. cis and trans forms of the hyponitrite dianion.

NO in liquid ammonia produces a solid that was later identified by IR spectroscopy as *cis*-$Na_2N_2O_2$.[86] Andrews and co-workers have prepared several such hyponitrite salts from the reactions of laser-ablated metals with NO at 4−7 K in inert gas matrices.[87−89] Sodium hyponitrite can also be prepared from the chemical reduction of sodium nitrite.[90] The reaction of N_2O with Na_2O generates the *cis*-$Na_2N_2O_2$ compound identified by X-ray structural analysis.[91−93] Bohle and co-workers have prepared and characterized a series of organic soluble hyponitrite salts of the form $[organic]^{2+}[N_2O_2]^{2-}$ and determined their X-ray crystal structures; they also determined the crystal structure of *trans*-$Na_2N_2O_2$.[94]

Coordination Compounds. A few transition-metal hyponitrite compounds have been reported in the literature, and these are generally prepared by (i) coupling of two NO molecules by metal complexes[95,96] (ii) coupling of chemisorbed NO metal surfaces,[97−99] (iii) attack of NO on a metal−NO group,[100−102] and (iv) transfer of the hyponitrite moiety from an organic diazenium diolate to a metal.[103,104] The binding modes of hyponitrites in transition-metal complexes that have been structurally characterized by X-ray diffraction are shown in Figure 23. The *cis*-hyponitrite binding mode to a single metal (structure **A**) has been demonstrated for the complexes $(PPh_3)_2Pt(N_2O_2)$[104,105] and (dppf)Ni(N_2O_2) [dppf = 1,1′-bis(diphenylphosphanyl)ferrocene].[103]

(76) Mckellar, A. R. W.; Watson, J. K. G.; Howard, B. J. *Mol. Phys.* **1995**, *86*, 273–286.
(77) Byl, O.; Kondratyuk, P.; Yates, J. J. T. *J. Phys. Chem. B* **2003**, *107*, 4277–4279.
(78) Zhao, Y.-L.; Bartberger, M. D.; Goto, K.; Shimada, K.; Kawashima, T.; Houk, K. N. *J. Am. Chem. Soc.* **2005**, *127*, 7964–7965.
(79) Fuster, F.; Dezarnaud-Dandine, C.; Chevreau, H.; Sevin, A. *Phys. Chem. Chem. Phys.* **2004**, *6*, 3228–3234.
(80) Taguchi, N.; Mochizuki, Y.; Ishikawa, T.; Tanaka, K. *Chem. Phys. Lett.* **2008**, *451*, 31–36.
(81) Snis, A.; Panas, I. *Chem. Phys.* **1997**, *221*, 1–10.
(82) Dutton, A. S.; Fukuto, J. M.; Houk, K. N. *Inorg. Chem.* **2005**, *44*, 4024–4028 [Erratum: pp 7687−7688].
(83) Poskrebyshev, G. A.; Shafirovich, V.; Lymar, S. V. *J. Am. Chem. Soc.* **2004**, *126*, 891–899.
(84) Poskrebyshev, G. A.; Shafirovich, V.; Lymar, S. V. *J. Phys. Chem. A* **2008**, *112*, 8295–8302.
(85) Andrews, L.; Zhou, M. F.; Willson, S. P.; Kushto, G. P.; Snis, A.; Panas, I. *J. Chem. Phys.* **1998**, *109*, 177–185.
(86) Goubeau, J.; Laitenberger, K. *Z. Anorg. Allg. Chem.* **1963**, *320*, 78–85.
(87) Andrews, L.; Liang, B. *J. Am. Chem. Soc.* **2001**, *123*, 1997–2002.
(88) Andrews, L.; Wang, X.; Zhou, M.; Liang, B. *J. Phys. Chem. A* **2002**, *106*, 92–95.
(89) Andrews, L.; Citra, A. *Chem. Rev.* **2002**, *102*, 885–911.
(90) McGraw, G. E.; Bernitt, D. L.; Hisatsune, I. C. *Spectrochim. Acta* **1967**, *23A*, 25–34.
(91) Feldmann, C.; Jansen, M. *Angew. Chem., Int. Ed. Engl.* **1996**, *35*, 1728–1730.
(92) Feldmann, C.; Jansen, M. *Z. Anorg. Allg. Chem.* **1997**, *623*, 1803–1809.
(93) Feldmann, C.; Jansen, M. *Z. Kristallogr.* **2000**, *215*, 343–345.
(94) Arulsamy, N.; Bohle, D. S.; Imonigie, J. A.; Sagan, E. S. *Inorg. Chem.* **1999**, *38*, 2716–2725.
(95) Bottcher, H.-C.; Graf, M.; Mereiter, K.; Kirchner, K. *Organometallics* **2004**, *23*, 1269–1273.
(96) Cenini, S.; Ugo, R.; La Monica, G.; Robinson, S. D. *Inorg. Chim. Acta* **1972**, *6*, 182–184.
(97) Lorenzelli, V.; Busca, G.; Sheppard, N.; Al-Mashta, F. *J. Mol. Struct.* **1982**, *80*, 181–186.
(98) Ramprasad, R.; Hass, K. C.; Schneider, W. F.; Adams, J. B. *J. Phys. Chem. B* **1997**, *101*, 6903–6913.
(99) Azambre, B.; Zenboury, L.; Koch, A.; Weber, J. V. *J. Phys. Chem. C* **2009**, *113*, 13287–13299.
(100) Franz, K. J.; Lippard, S. J. *J. Am. Chem. Soc.* **1999**, *121*, 10504–10512.
(101) Gwost, D.; Caulton, K. G. *Inorg. Chem.* **1974**, *13*, 414–417.
(102) Schneider, J. L.; Carrier, S. M.; Ruggiero, C. E.; Young, V. G.; Tolman, W. B. *J. Am. Chem. Soc.* **1998**, *120*, 11408–11418.
(103) Arulsamy, N.; Bohle, D. S.; Imonigie, J. A.; Levine, S. *Angew. Chem., Int. Ed.* **2002**, *41*, 2371–2373.
(104) Arulsamy, N.; Bohle, D. S.; Imonigie, J. A.; Moore, R. C. *Polyhedron* **2007**, *26*, 4737–4745.
(105) Bhaduri, S.; Johnson, B. F. G.; Pickard, A.; Raithby, P. R.; Sheldrick, G. M.; Zuccaro, C. I. *J. Chem. Soc., Chem. Commun.* **1977**, 354–355.

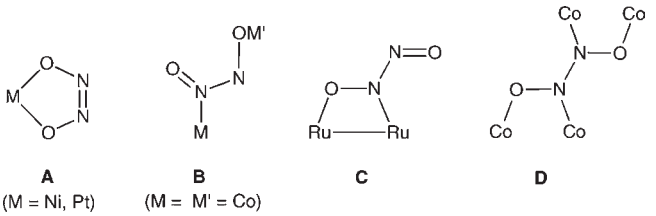

Figure 23. Structurally characterized metal hyponitrite binding modes in inorganic coordination compounds.

A *cis*-hyponitrite N,O-binding mode (structure **B**) has been established for the bimetallic cation $[(NH_3)_5Co(\mu\text{-}N_2O_2)Co(NH_3)_5]^{4+}$.[106,107] The structure **C** that contains a *trans*-hyponitrite N,O-binding mode was determined for the $Ru_2(CO)_4(\mu\text{-}H)(\mu\text{-}PBu^t_2)(\mu\text{-dppm})(\mu\text{-}N_2O_2)$ product obtained from the reductive dimerization of NO by its bimetallic ruthenium precursor $Ru_2(CO)_4(\mu\text{-}H)(\mu\text{-}PBu^t_2)(\mu\text{-dppm})$ (dppm = $Ph_2PCH_2PPh_2$).[95] The complex $[(NO)_2Co(\mu\text{-}NO_2)]_2(\mu\text{-}N_2O_2)$, isolated as a minor product from the reaction of $Co(CO)_3NO$ with NO, contains the tetradentate planar hyponitrite ligand sketched as structure **D**.[108]

Heme and Heme Models. The reduction of two molecules of NO to N_2O is a formal two-electron process (eq 2) that can be carried out by the bimetallic active sites in

$$2NO + 2H^+ + 2e^- \rightarrow N_2O + H_2O \qquad (2)$$

the heme-containing bacterial NO reductases (NORs).[109] In contrast, the fungal NORs contain a monometallic heme thiolate active site.[110] Lehnert and co-workers have provided an excellent theoretical treatment of NO reduction by the single metal center in a fungal NOR model.[111] Our emphasis in this article, however, is on NO reduction by bimetallic NORs.

In the active sites of the bacterial NORs, the heme (referred to as heme b_3) is in close proximity to a nonheme iron center (referred to as Fe_B), and current evidence suggests that both the heme and nonheme iron centers play active roles in the reduction of NO to N_2O. A major drawback in firmly establishing the mechanism(s) for the reduction of NO by NORs is that it has been difficult to identify intermediates along the NO reduction pathway. Three mechanisms are commonly discussed in the literature (Figure 24),[109] and all three involve the coupling of two NO molecules at a diferrous active site followed by the formation of a putative diferric hyponitrite intermediate prior to the release of N_2O and generation of the resting oxo-bridged diferric NOR (with an Fe-to-Fe separation of $\leq$3.5 Å in *Pd* cNOR).[109,112] Moënnez-Loccoz has provided a comprehensive treatise on the

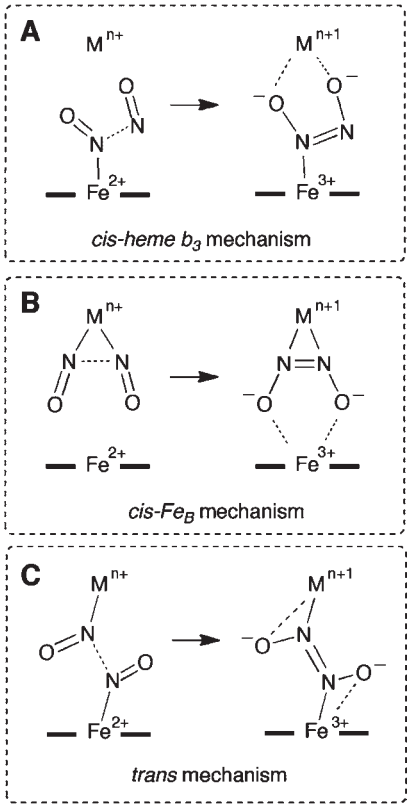

Figure 24. Intermediates in the three putative mechanisms for NO reduction by NORs and HCOs.

available experimental spectroscopic data that argue for one or more of the putative mechanisms shown in Figure 24.[109] The *cis*-heme b_3 mechanism involves attack of a second NO molecule on a heme $\{FeNO\}^7$ species to generate an asymmetrically bridged hyponitrite ligand. In the case of the *cis*-Fe_B mechanism, a nonheme dinitrosyl iron complex forms prior to NO coupling and hyponitrite formation. The trans mechanism presumes the formation of both heme and nonheme $\{FeNO\}^7$ moieties that couple via N−N bond formation.

The NORs are evolutionarily related to the heme copper oxidases (HCOs) that also contain bimetallic active sites.[113,114] In the case of HCOs, the heme (heme a_3) is in close proximity to a copper site (rather than a nonheme iron site as found in the NORs). Some prokaryotic HCOs such as cytochromes ba_3 and caa_3 from *Thermus thermophilus*, and cytochrome cbb_3 from *Paracoccus stutzeri* display NOR activities.[114]

Varotsis and co-workers have employed resonance Raman spectroscopy to identify an intermediate during the Tt ba_3 NOR reaction pathway that they assign to a bridged protonated hyponitrite compound **E** (Figure 25) that forms subsequent to the initial generation of a dinitrosyl heme−NO/CuNO species.[115] The proposed identity of this bridged hyponitrite compound is derived from DFT calculations (B3LYP functional; 6-31G* basis set)[116] and

(106) Hoskins, B. F.; Whillans, F. D.; Dale, D. H.; Hodgkin, D. C. *J. Chem. Soc., Chem. Commun.* **1969**, 69–70.
(107) Villalba, M. E. C.; Navaza, A.; Guida, J. A.; Varetti, E. L.; Aymonino, P. J. *Inorg. Chim. Acta* **2006**, *359*, 707–712.
(108) Bau, R.; Sabherwal, I. H.; Burg, A. B. *J. Am. Chem. Soc.* **1971**, *93*, 4926–4928.
(109) Moënne-Loccoz, P. *Nat. Prod. Rep.* **2007**, *24*, 610–620.
(110) Daiber, A.; Shoun, H.; Ullrich, V. *J. Inorg. Biochem.* **2005**, *99*, 185–193.
(111) Lehnert, N.; Praneeth, V. K. K.; Paulat, F. *J. Comput. Chem.* **2006**, *27*, 1338–1351.
(112) Moënne-Loccoz, P.; Richter, O.-M. H.; Huang, H.-W.; Wasser, I. M.; Ghiladi, R. A.; Karlin, K. D.; de Vries, S. *J. Am. Chem. Soc.* **2000**, *122*, 9344–9345.
(113) Pinakoulaki, E.; Varotsis, C. *J. Inorg. Biochem.* **2008**, *102*, 1277–1287.
(114) Zumft, W. G. *J. Inorg. Biochem.* **2005**, *99*, 194–215.
(115) Varotsis, C.; Ohta, T.; Kitagawa, T.; Soulimane, T.; Pinakoulaki, E. *Angew. Chem., Int. Ed.* **2007**, *46*, 2210–2214.
(116) Ohta, T.; Kitagawa, T.; Varotsis, C. *Inorg. Chem.* **2006**, *45*, 3187–3190.

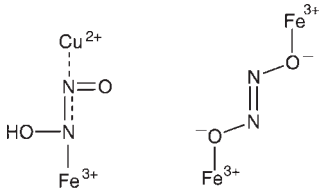

Figure 25. Proposed intermediate (**E**) and a structurally characterized (**F**) bimetallic heme hyponitrite moiety.

from bands in the resonance Raman spectra at 626 and 1334 cm^{-1} that they assign to the heme a_3 Fe−N−OH bending and the N−N stretching vibrations, respectively;[115] the lower N−N stretching vibration (cf. free hyponitrite at 1392 cm^{-1})[87] suggests less double-bond character in the proposed structure **E**.

Blomberg and co-workers have performed DFT calculations (B3LYP functional) to probe the likely mechanisms of NOR activity in a bacterial NOR model[117] and in a ba_3-type HCO.[118] Their results appear to favor attack of a second NO molecule on a heme b_3 (NOR) or heme a_3 (HCO) $\{FeNO\}^7$ species (i.e., the *cis*-heme b_3 mechanism in Figure 24, where M = Fe in NOR and M = Cu in HCO).

Clearly, bioinorganic chemistry has a vital role to play in helping to elucidate the coordination and reaction chemistry of heme hyponitrites. For example, Lu and co-workers have engineered a copper binding site into the distal pocket of Mb and have clearly demonstrated that this Cu_BMb mutant catalyzes the reduction of NO to N_2O.[119] Importantly, they have also engineered an Fe^{II} binding site into Mb, and this Fe_BMb mutant displays a ~10-fold faster NO reduction activity than the Cu_BMb mutant.[120] Collman and co-workers have utilized the results from the reaction of a functional diferrous synthetic model of the active site of NOR with NO to propose that a *trans*-dinitrosyl intermediate forms (i.e., the trans mechanism in Figure 24) at the active site of NOR followed by NO coupling to give N_2O and a diferric product.[121,122] The heme and nonheme nitrosyl intermediates were characterized spectroscopically at low temperatures. Karlin and co-workers have provided clear evidence that a synthetic heme/copper model of HCO will also reductively couple NO to N_2O in the presence of acid, thus substantiating the requirement for both metal and acid for this NOR reaction to occur.[123]

Our research into hyponitrites stems from our interest in designing tractable compounds that can be used to study the coordination chemistry of hyponitrites in a systematic fashion. Prior to our work in this area, there were no crystallographically characterized heme or heme model hyponitrites. We thus set out to prepare an isolable heme hyponitrite compound that we would subject to crystallization efforts and structure solution. The reaction of the oxo-bridged dimer $[(OEP)Fe]_2(\mu\text{-}O)$ with hyponitrous acid (eq 3) gave, after workup, a stable hyponitrite-bridged iron porphyrin product in good yield.[124]

$$[(OEP)Fe]_2(\mu\text{-}O) + H_2N_2O_2 \rightarrow [(OEP)Fe]_2(\mu\text{-}N_2O_2) + H_2O \quad (3)$$

A band at 982 cm^{-1} in the IR spectrum of the product was assigned to ν_{as} of the NO group ($\nu_{as}(^{15}NO)$ 973 cm^{-1}). The X-ray crystal structure of this compound is shown in Figure 26. The compound crystallizes as a tetrakis(dichloromethane) solvate, where the CH_2Cl_2 molecules surround the hyponitrite bridge. Figure 26 (top) shows the molecule without the CH_2Cl_2 solvates. As is seen in the figure, the hyponitrite ligand is bound to each Fe atom via the η^1-O binding mode, and the hyponitrite ligand is trans (i.e., structure **F** in Figure 25). The N−N bond length of 1.250(3) Å is indicative of double-bond character (cf. 1.256(2) Å in *trans*-$Na_2N_2O_2$)[94] and suggests substantial hyponitrite (i.e., dianionic) character to this bridging ligand. DFT calculations were performed for geometry optimization for the porphine analogue $[(por)Fe]_2(\mu\text{-}N_2O_2)$ using the BLYP functional with a TZP basis set and a frozen core for all atoms and for subsequent single-point energy calculations using the B3LYP functional and an all-electron TZP basis set. The DFT calculations on the porphine analogue reveal that the calculated geometry of a ferric high-spin *trans*-N_2O_2 system most closely reproduces the crystal structural data, consistent with the electron paramagnetic resonance data for the product as a CH_2Cl_2/toluene glass at 77 K.[124] The frontier spin orbitals from the unrestricted open-shell calculations (shown in Figure 27) reveal that the N atoms of the hyponitrite bridge form a bonding interaction in both highest occupied spin orbitals. The detailed magnetic behavior of this complex remains to be explored, however.

We then explored the possibility of N_2O generation from this complex. The addition of hydrochloric acid to the hyponitrite-bridged complex results in the formation of N_2O and (OEP)FeCl (eq 4).

$$[(OEP)Fe]_2(\mu\text{-}ONNO) + 2HCl \rightarrow N_2O + 2(OEP)FeCl + H_2O \quad (4)$$

N_2O was identified by IR spectroscopy of the headspace; new bands at 2236/2213 and 1298/1266 cm^{-1} were attributed to ν_{as} and ν_s of N_2O, respectively.[125,126] Use of the ^{15}N-labeled hyponitrite shifts the ν_{as} bands to 2167/2144 cm^{-1}; the corresponding ν_s bands were not observed because of their occurrence outside the detection window.

(117) Blomberg, L. M.; Blomberg, M. R. A.; Siegbahn, P. E. M. *Biochim. Biophys. Acta* **2006**, *1757*, 240–252.
(118) Blomberg, L. M.; Blomberg, M. R. A.; Siegbahn, P. E. M. *Biochim. Biophys. Acta* **2006**, *1757*, 31–46.
(119) Zhao, X.; Yeung, N.; Russell, B. S.; Garner, D. K.; Lu, Y. *J. Am. Chem. Soc.* **2006**, *128*, 6766–6767.
(120) Yeung, N.; Lu, Y. *Chem. Biodiversity* **2008**, *5*, 1437–1454.
(121) Collman, J. P.; Dey, A.; Yang, Y.; Decreau, R. A.; Ohta, T.; Solomon, E. I. *J. Am. Chem. Soc.* **2008**, *130*, 16498–16499.
(122) Collman, J. P.; Yang, Y.; Dey, A.; Decreau, R. A.; Ghosh, S.; Ohta, T.; Solomon, E. I. *Proc. Natl. Acad. Sci. U.S.A.* **2008**, *105*, 15660–15665.
(123) Wang, J.; Schopfer, M. P.; Sarjeant, A. A. N.; Karlin, K. D. *J. Am. Chem. Soc.* **2009**, *131*, 450–451.
(124) Xu, N.; Campbell, A. L. O.; Powell, D. R.; Khandogin, J.; Richter-Addo, G. B. *J. Am. Chem. Soc.* **2009**, *131*, 2460–2461.
(125) Captain, D. K.; Amiridis, M. D. *J. Catal.* **2000**, *194*, 222–232.
(126) Nightingale, R. E.; Downie, A. R.; Rotenberg, D. L.; Crawford, B.; Ogg, R. A. *J. Phys. Chem.* **1954**, *58*, 1047–1050.

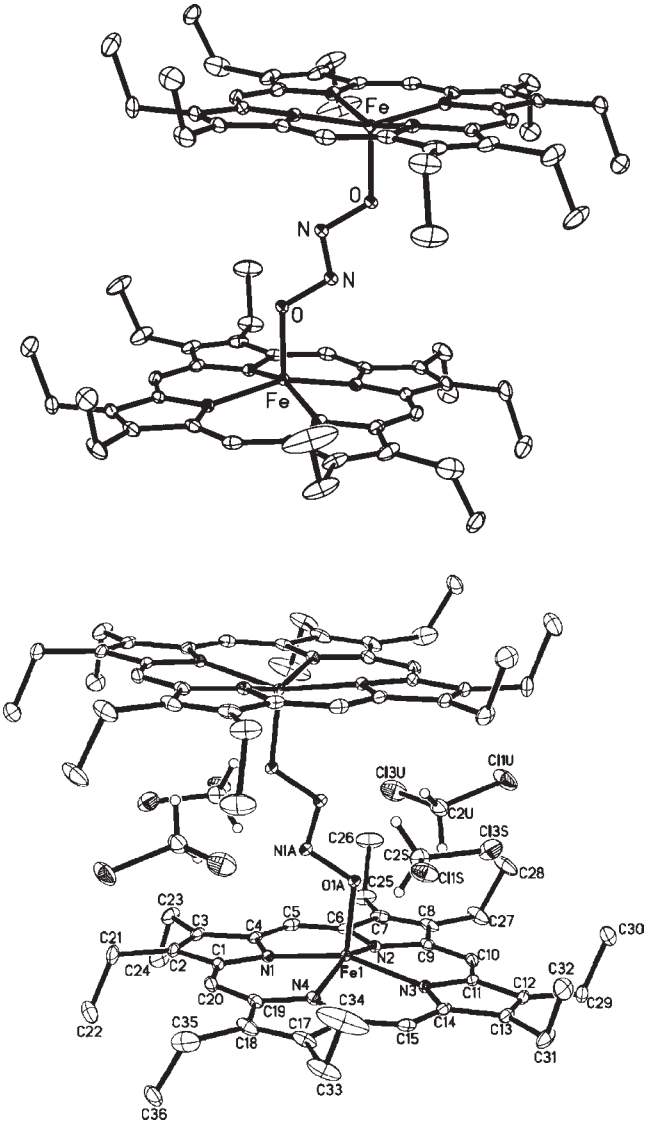

Figure 26. Molecular structure of $[(OEP)Fe]_2(\mu\text{-ONNO})$. Top: H atoms and the CH_2Cl_2 solvates have been omitted for clarity. Bottom: With CH_2Cl_2 solvates but without nonsolvate H atoms. Selected bond lengths (Å) and angles (deg): Fe−O = 1.889(2), O−N = 1.375(2), N−N = 1.250(3), Fe−N(por) = 2.049(2)−2.064(2), ∠FeON = 118.56(12), ∠NNO = 108.5(2). Reproduced from ref 124. Copyright 2009 The American Chemical Society.

The successful preparation of this $[(OEP)Fe]_2(\mu\text{-ONNO})$ complex is only the beginning of what could be a fruitful area of research into heme hyponitrites. However, we note that the O,O binding of the hyponitrite in this complex might be possible because of the generous Fe−Fe distance of 6.7 Å in this complex (i.e., it can accommodate an O,O-binding mode). This 6.7 Å distance is longer than the 4.4 Å distance between the iron and copper centers in *T. thermophilus* cytochrome ba_3 that exhibits NOR activity.[127] Ongoing work in our laboratories is centered on the design and preparation of iron porphyrin hyponitrite complexes exhibiting different binding modes of the hyponitrite ligand (e.g., a possible N-binding mode in a ferrous derivative) and exploring the differences in the chemical reactivities of the hyponitrite linkage isomers.

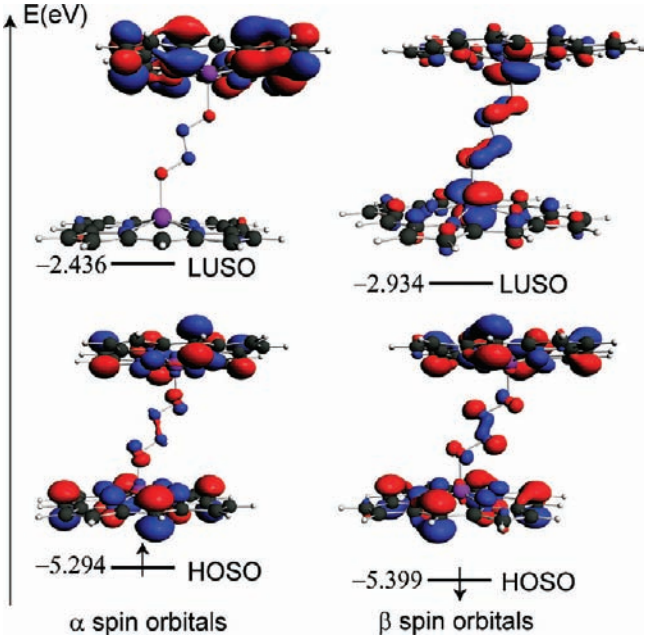

Figure 27. Frontier spin orbitals for high-spin $[(porphine)Fe]_2(\mu\text{-ONNO})$. HOSO and LUSO denote the highest occupied and lowest unoccupied spin orbitals, respectively. Reproduced from ref 124 Copyright 2009 The American Chemical Society.

Conclusions

To a large extent, the study of linkage isomerization in heme−NOx compounds is still in its infancy. It is possible that the intense coloration of nitrosyl metalloporphyrins hinders efficient light penetration for obtaining high yields of the photogenerated isonitrosyl (η^1-ON) and/or side-on (η^2-NO) linkage isomers starting from their ground-state nitrosyl precursors. Their demonstrated existence, however, in synthetic iron porphyrins suggests that they cannot be readily ignored in discussions about heme−NO interactions. Indeed, a recent calculation on Mb(NO) suggests the possible existence of the metastable Mb(η^1-ON) linkage isomer in this protein.[128] Clearly, more work needs to be done to elucidate any contributions such linkage isomers may make toward the overall biological activity of NO. In the case of nitrite binding, the existence of its N and O binding to heme proteins provides an entry into studies that may differentiate between the nitrite reductase activities of the proteins as a function of the nitrite binding mode. Only one synthetic metalloporphyrin hyponitrite compound has been reported to date.

We fully expect that synthetic bioionorganic chemistry of heme−NOx compounds will continue to play an important role in delineating the rather diverse roles that NO plays in mammalian physiology.

Acknowledgment. We are grateful to the National Institutes of Health (Grant GM064476) and the Oklahoma Center for the Advancement of Science and Technology (Grant HR09-081) for funding of this work.

(127) Soulimane, T.; Buse, G.; Bourenkov, G. P.; Bartunik, H. D.; Huber, R.; Than, M. E. *Embo J.* **2000**, *19*, 1766–1776.

(128) Nutt, D. R.; Karplus, M.; Meuwly, M. *J. Phys. Chem. B* **2005**, *109*, 21118–21125.